Coupled Partition and Configuration for Cohesive and Self-sufficient Virtual Microgrids

Lechuan Piao, Fei Xue*, Shaofeng Lu, Lin Jiang, Xiaoliang Wang and Qigang Wu

***Abstract*—Active Distribution Network shows promise in operating and controlling distributed generations. Based on ADN structural and electrical differences, ADN could be partitioned to reveal innate heterogeneity for better control. Virtual Microgrid works as such a partition mode that each VM serves both as a part of ADN and as an individual operating agent. To identify VM boundaries, previous research utilized community detection methods and then configured ADN based on stationary partition. In this paper, VM partition and configuration are simultaneously determined in the proposed Coupled-Configuration-Partition of Active Planning. Also, a new definition of electrical edge betweenness is proposed to depict interaction among power system buses to improve the partition algorithm. Based on this proposal, ADN is planned to be cohesive in Net-ability, Flexibility Supply Index, and Capacity Fitness, in the meantime to minimize the cost in a multi-objective optimization, iteratively in Genetic Algorithm to reach Pareto Front. Case studies are designed to denote the benefits of the proposed Coupled-Configuration-Partition of Active Planning in modularity and system cohesion intensity.**

***Index Terms*—Active Planning, Complex Networks, Virtual Microgrids, Electrical Edge Betweenness, Flexibility Quantification**

1. Introduction

The idea of Active Distribution Network (ADN) was formed up in [1] by S. Chowdhury *et al.* to actively control distribution networks' behaviour, by integrating Distributional Energy Resources (DER) and introducing Distributed Generators (DG), Distributed Energy Storage Systems (DESS), and corresponding Supervisory Control And Data Acquisition (SCADA) in a network with bi-directional power flow setting. This notion only covers grid management phase, in its original definition.

However, to build ADN in reality, the first task is to develop a reasonable and effective plan. Optimal planning is a well-researched area, trying to find the optimal configuration for certain systems. However, in ADN planning, only static optimal value is not enough. Similar to clarifying the idea from a vague notion *smart grid* to specific *active distribution network*, the idea of *active planning* is proposed as revision to *optimal planning*.

In active planning, the optimization process must account for the variation of systems, both *temporally* and *spatially*. In this paper, temporal assessment, such as wind/load prediction and Renewable Energy Sources (RES) generation, is carried out by time-related sampling points in Monte-Carlo Simulation (MCS). With more adequate sampling of a scenario space, the planning result would be based on more comprehensive scenarios. For spatial evaluation, we introduced complex network theory in active planning. Different nodes and branches in ADN have different importance. Through network analysis, we can utilize such differences and then discover the hidden features of the network.

One of most important spatial-related issues is partitioning of ADN. Some nodes are intensively connected with their neighbours via feeders, whereas some other branches provide lesser supports, albeit necessary, in power transmission. Hence, in order to detect communities in ADN, Electrical Edge Betweenness (EEB) is introduced and calculated for active planning in this paper. Based on edge betweenness, Newman *et al.* proposed [2] the well-received Girvan-Newman Algorithm (GNA) for community detection and partitioning, considering the network as a graph. By iteratively removing lines with highest betweenness and choosing the number of partitions with highest modularity, GNA can produce a dendrogram containing graph partition for further analysis. Based on GNA, in our research, Inversed Girvan-Newman Algorithm (IGNA) is proposed and used for ADN partitioning.

For operation of partitioned distribution networks, previous research exploited the network attributions of ADN to enhance system performance. In [3], Biserica *et al.* proposed K-mean clustering for steady voltage control. In [4], Chai *et al.* proposed Tabu search, applied on voltage sensitivity based on modularity proposed by Girvan and Newman [2] for voltage coordination control under high PV penetration. In [5], Ruan *et al.* proposed a novel method similar to Girvan-Newman Method, only to use the variation of electrical distance and power balance indicators as the betweenness. In [6], voltage control of ADN are coupled with dynamic network partition leading to better efficiency, but the number of partition is arbitrarily assigned, without proper assessment of partition. The idea of complex system partition can even be extended to more features in power system. In [7], researchers applied complex network analysis across physical,

Lechuan Piao and Fei Xue* are with the Department of Electrical and Electronic Engineering, Xi'an Jiao Tong-Liverpool University, Suzhou, Jiangsu Province, 215123, China (e-mail: lechuan.piao@liverpool.ac.uk, fei.xue@xjtlu.edu.cn)

Shaofeng Lu is with the Shien-Ming Wu School of Intelligent Engineering, South China University of Technology (e-mail: lushaofeng@scut.edu.cn)

Lin Jiang is with the Department of Electrical Engineering and Electronics, University of Liverpool, Liverpool, Merseyside L69 3BX, UK (e-mail: l.jiang@liverpool.ac.uk)

Xiaoliang Wang is with the School of Electronic and Information Engineering, Suzhou University of Science and Technology, and Jiangsu Industrial Intelligent and Low-carbon Technology Engineering Centre, Suzhou, China. (e-mail: xiaoliang.wang@usts.edu.cn)

Qigang Wu is with the School of Electrical and Automation, Changshu Institute of Technology, Jiangsu Province, 215506, China (e-mail: qigangw@cslg.edu.cn)

*Corresponding Author

cyber, socioeconomics, and environment layers, yielding more stable result under RES fluctuation. The structure of microgrids can also be built upon ADN partition. In [8], E. Nassar et al. used dynamic boundaries for self-adequate microgrids partitioning in ADN operational stage, but the DG allocations are given as an input, instead of dynamically determined.

In conventional optimal planning with system partitioning, the partition process may happen either before or after the allocation of system components. For example, in [9], optimal allocation of renewables and DESS are based on previous static partition results from ECS and Electrical Modularity, which only considers line impedance but not integrating influence from dynamic planning results. On the contrary, M. Barani et al. [10] used optimal partitioning in constructing supply-sufficient microgrids, with the resources are limited to reclosers and DESS, in which the partition process happens after the configuration is determined. We named the one with prerequisite boundary as Predefined Boundary Active Planning (PBAP), and the system partition with a priori configuration information are called Predefined Configuration Partition (PCP).

Compared with PCP, PBAP method is beneficial for Distribution System Organizers (DSO) without the authority or ability to deploy DES immediately. For example, microgrid organizers can purchase the right of managing and gaining profits from certain cluster of buses based on predefined boundary, even before ADN is fully developed. PBAP enables DSOs to gain investment to purchase and install ADN assets gradually based on fixed boundaries.

One major difference between PBAP and PCP is the utilization of system's spatial information in partition and configuration process. In PBAP, configuration is based on spatial information on system partition, but partition process is based on incomplete information of an empty network, neglecting the graph variation caused by configuration. PCP could be suitable for preliminary development of ADN where DES were developed disorderly, and the partition passively consider DES configuration as given conditions. ¬

However, there is a lack of research in active planning based on both the information by ADN configuration and partition. Since the allocation of DGs and DESSs can affect the graphical representation of ADN, active planning based on static graph will lead to negligence of the modified system edge weights.

In this paper, we proposed Coupled-Configuration-Partition of Active Planning (CCP-AP), which is a combined process of both system graph partition and optimal planning. This is proposed to determine power system assets' optimal allocation, such as DG and DESS, and ADN partitions alternately. CCP-AP use dynamic representation during the exec¬¬¬¬ution, improved the accuracy of active planning.

Another salient point of the benefits in CCP-AP is the ability of combining optimal distribution network built or expansion, e.g., additional feeders, substations, and Soft Open Points (SOP) installations, with active planning process, because the CCP-AP can incorporate the variation of graph structure during the execution of algorithm. When original distribution is structurally modified, CCP-AP simultaneously determines the optimal partition for the new topology, which will not achieved by optimal planning with predefined and static boundary.

Virtual Microgrid (VM) is a concept that ADN components are partitioned and managed as microgrids, without the need for physical ADN separation. It utilizes existing DN infrastructure and has the technology edge in many aspects, including community detection and decentralized control. Compared with Virtual Power Plant (VPP), VM focuses on not only the generation and management of power, but also cooperative or competitive interplay among VMs, which means VM serves as smart agents in distributive optimization problems such as energy trading, situational awareness, etc.

Spatial features play more critical roles in multiple VMs operation than VPPs. In past research [11-13],VM is created in clustering CDN for system performance optimization, without considering the but only the supply demand balance. Based on a complex network method, the boundary of VM can be identified by structural characteristics [14] so that each VM may perform with better efficiency. In this paper, the novel CCP-AP method will be applied in VM setting. The ADN will be viewed as graph and VMs as subgraphs, thus proposed method can utilize both temporal and spatial features in optimal planning.

Based on structural community detection, the idea of cohesion is brought up to interpret the relationship among VMs and ADN. Generally, for a multiple-subsystems network, one subsystem will be cohesive if its certain feature is better than the whole. In this research, the cohesion of system Flexibility Supply Index (FSI) and Revised Net-Ability (RNA) will be considered in optimization.

Flexibility Supply Index is designed as the norm of an array in which ramp rate, power capacity and energy capacity, both upwards and downwards, are compared between flexibility supplies and uncertainty. In this paper, uncertainty is viewed as the load of flexibility. For flexibility quantification, many methods were given in past literatures. In [15], upwards/downwards flexibility is distinguished for evaluating flexibility metrics in unit commitment and availability in transmission networks. In [16], J. Ma *et al.* averaged power capacity and ramp rate, without considering energy. In [17], K. Studarus *et.al* proposed stochastic operational flexibility, focusing on very short term flexibility and distinguished controllable and uncontrollable power resources, and the latter is defined as uncertainty. In [18], Y. Makarov *et al.* first proposed using energy capacity, ramp rate, and duration to estimate operational impact. In [19], the triad of ramp rate, power, and energy is used by Ulbig *et al.* to calculate operational flexibility both upwards and downwards using Minkowski Summation. In [20], Bucher et al. used the same quantification triad and extended to locational flexibility of power system devices at different buses. In this paper, flexibility array containing the triad of ramp rate, power, and energy both upwards and downwards will be considered in a very short time, i.e., 15 min for system forecast and devices' reaction. Our proposed flexibility array can apply both to system and to devices.

RNA is the indicator of self-sufficiency and network aptitude. Net-Ability (NA) derives from graph efficiency [21] and Revised NA depicts electrical distance, considering equivalent impedance. Those two ideas will be further explained in Section 3.

This paper is structured as such: Section 2 makes a general discussion on important concepts in this paper, including ADN

framework, VM, Self-Sufficiency, Cohesion, and Partition; Section 3 introduces the IGNA and a bi-level multi-objective optimization algorithm's design and implementation; Section 4 shows the case study based on IEEE PG&E 69 bus distribution system. In Section 5, a discussion is made upon the technical and market realization of VM and CCP-AP process. Section 6 concludes this paper.

2. Virtual Microgrid Related Concepts

2.1. Active Planning, Management, and Defence

To implement ADN, three critical characteristics are proposed as active planning, active management, and active defence.

As mentioned in Section 1, active planning is one optimal planning process in which temporal and spatial dynamic features are comprehensively considered.

Active management denotes the coordinated control of ADN and its subsystems. Due to the introduced fluctuating RES, issues may occur in voltage stability, frequency stability, system observability, power balance, etc. In ADN, Transactive Energy System (TES) should also be enabled, using the marketized electricity for system clearance and reduce RES curtailment.

Traditionally, distribution networks adopted this strategy of *fit-and-forget* in constructing resources. The management process and planning process works normally independently, and the planning process will allow a large amount of redundancy. However, in active planning and active management, the coupling of operation and planning is essential [22]. For example, because of higher level of uncertainties in ADN than conventional distribution network, active planning shall quantify and introduce more flexibility sources to counterpart the uncertainty. On the other hand, active management shall form up better policies and strategies for ADN control and flexibility supply scheduling.

Active Defence is the process preventing cascading failures and malicious attacks on ADN, including techniques like false data injection attack detection, defence capacity maximization, situational awareness, etc. Active planning serves as the cornerstone of active management and defence, as it must give comprehensive consideration about temporal factor throughout the whole lifespan in ADN, including management and defence. Specifically, management capability and defence capability are to be considered in active planning optimization process.

2.2. Virtual Microgrid Self-Sufficiency

Self-sufficiency, or self-adequacy, refers to the ability of VM to work independently in island mode. Conventionally, self-sufficiency refers to static power balance between demand and supply, often represented by the ratio between total load and installed generation capacity [8, 12].

In our research, self-sufficiency is extended to present Capacity Fitness (CF) and flexibility supply in both active management and defence. The mathematical definition will be given in Section 4.3. CF estimates how much critical load can be supplied in each VM in islanding mode, and flexibility supply targets at system uncertainty. CF targets at power supply installed, and flexibility supply depicts power available in real time, dealing with unforeseeable uncertainty. They both constitute what we call self-sufficiency.

Flexibility supply is quantified by Flexibility Supply Index (FSI). It addresses the risk of system imbalance due to forecast errors. In a large RES penetration setting especially, FSI is more important to prevent potential lack of power, ramp rate, and energy.

2.3. Cohesion

For VMs in the whole ADN, they jointly work as subsystems in an integrated system. Ideally, a smart subsystem partition method should generate partitions showing better characteristics than the whole. A subsystem is deemed cohesive, if and only if,

$$c(s) > c(\mathcal{S}), \qquad s \in \mathcal{P} \tag{1}$$

where $c(s)$ is the characteristic to be considered in subsystem s and $c(\mathcal{S})$ is measuring of whole system $\mathcal{S}$. $\mathcal{P}$ is the set containing partition information.

An illustration of cohesion is shown in Fig 1. In Fig 1. (a), adjacent nodes have the same geodesic distance as 1 meter, thus the system is showing homogeneity instead of heterogeneity. In Fig 1. (b) on the contrary, with any subsystems in $\mathcal{P}$, the circled nodes have much closer average geodesic distances (1m) than the average distance of the whole system (34m). Thus, those four subsystems, differentiated by colours, are viewed as cohesive.

Thus, we define Cohesion Intensity (CI) as such:

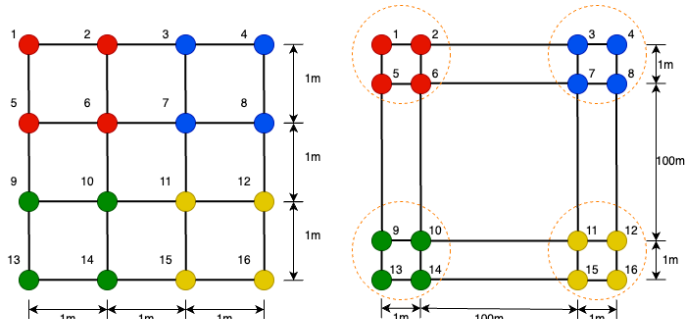

Fig. 1 Cohesion of Subsystems

$$CI(\mathcal{S}) = \frac{1}{N_s}\sum c(s) - c(\mathcal{S}), s_i \in \mathcal{P} \tag{2}$$

in which $CI(\mathcal{S})$ is calculated by the sum of cohesion feature c difference between whole system $\mathcal{S}$ and subsystem s. N_s is the number of subsystems in $\mathcal{S}$ and s_i is the i_{th} subsystem according to partition method $\mathcal{P}$.

2.4. CCP-AP with Betweenness

Active management benefits from partitioned ADN in active planning. By exploring system difference, system operator can implement regional control scheme. Moreover, transactive energy management can also be based on networked multiple microgrids, and by extension VM, as the smart agent [23, 24].

Partitioning ADN to subsystems also allows regional active defence. It helps to isolate faults and limit the impact of power outages by dividing the network into smaller sections.

Traditionally, there exists two serial types of planning process, which are community-detection-first and resource-allocation-first. In resource-allocation-first mechanism [8], planning process does not have partitioned information. In community-

detection-first mechanism, such as [9, 10], community detection is not based on information on different configuration the result may yield.

Thus, the process of ADN partitioning and resources allocation need to be coupled in planning, because the optimal allocation depends on the definition of VM boundary to calculate its fitness. On the other hand, the calculation of feeders' weights in ADN graph for partitioning is also dependent on the DER allocation. CCP-AP process allows more accurate partition and configuration of optimal planning.

Traditionally, Edge Betweenness (EB) is defined as the number of shortest paths between any pair of nodes in a graph G that pass through the edge. It is a measure of centrality that quantifies the importance of edges in graph. The edge with highest EB value is viewed as a bridge between large communities and maintains the connectivity of the graph. Originally in [25], Girvan and Newman proposed the idea of using edge betweenness for finding community structure in social and biological networks.

However, conventional definition of EB has no consideration in electrical features. Lines with different power limit and impedance may have identical EB. Also, conventional EB cannot distinguish different ADN configurations and load locations since all buses are viewed of the same importance. Researchers proposed centrality betweenness targeting at modelling power grids. In [26], P. Hines et.al proposed the idea of using electrical centrality for indicating electrical topology instead of physical topology, using the equivalent impedance matrix Z_{ij}. In [27], Wang et.al examined the different types of centrality betweenness and identified important nodes in power system. In this research, electrical edge betweenness is re-defined to denote line capacities and line impedance, which will be further explained in Section 3.1.

3. Algorithm Design

3.1. Electrical Edge Betweenness

Different from graph traversing problem, electricity flow is not only transferred through the shortest path, and it is intuitive that the power transfer distribution factor (PTDF) should be used for calculating the connection strength among electrical nodes. Inspired by [28], we define Electrical Edge Betweenness (EEB) as,

$$EEB(l) = \frac{(T^p(l) + |T^n(l)|)}{2} \tag{3}$$

$$T^p(l) = \sum_{g\in G}\sum_{d\in D}\frac{C_g^d f_l^{gd,+}}{Z_{gd}} \tag{4}$$

$$T^n(l) = \sum_{g\in G}\sum_{d\in D}\frac{C_g^d f_l^{gd,-}}{Z_{gd}} \tag{5}$$

in which $f_l^{gd,+}$ and $f_l^{gd,-}$ are the positive and negative elements of f_l^{gd}, which is the PTDF from generator g to load d on branch l. G and D are sets of generators and loads in ADN. $T^p(l)$ is the positive line betweenness and $T^n(l)$ is the negative line betweenness of branch l. Z_{ij} is the equivalent impedance from bus i to bus j.

In ADN, bi-directional power flow is allowed for flexibility issues. Thus, to consider $T^p(l)$ and $T^n(l)$ equally, the result of edge betweenness is averaged.

The distance between any pairs of vertices can be defined as the cost or difficulty in transmitting physical quantities [28]. Z_{gd} depicts the difficulty in transmitting electrical power between bus g and bus d. Conventionally, when calculating betweenness, each pair of g and d is treated equally and the electrical distance is not calculated between nodes. However, in power scheduling process, the possibility of system utilizes a far-away resource to cope with a local power imbalance situation is lower due to cost and stability issues. This idea shall lead to a lower value of designed EEB, since in-community collaboration shall be easier that outside community.

C_g^d is the power transmission capacity, defined as the maximal injection at bus g extracted at bus d. P_l^{max} is the maximum allowed active power flow in branch l. Power transmission capacity is limited by the weakest branch, thus the minimal value of power flow limit divided by PTDF is defined as power transmission capacity.

$$C_g^d = \min_{l\in L}\left(\frac{P_l^{max}}{\left|f_l^{gd}\right|}\right) \tag{6}$$

Conventionally, modularity is a systematic measurement that reflects in-community interactions, based on the idea that the sum of difference between the actual and the expected value of number of edges between two nodes [2]. The expected edge numbers are calculated according to random connections.

$$Q = \frac{1}{2m}\sum_{v,w}[A_{v,w} - \frac{k_v k_w}{2m}]\cdot\delta(C_v, C_w) \tag{7}$$

$$m = \frac{1}{2}\sum_{v,w}A_{v,w} \tag{8}$$

In above definition, $A_{v,w}$ is at the v_{th} row and w_{th} column in matrix A, the adjacency matrix. k_v and k_w are degree of node v and w. C_v and C_w is the community contains node v and w, and the Kronecker delta function makes sure only nodes pair in one community is selected. When node v and w are in the same community, $\delta(C_v, C_w) = 1$, otherwise 0.

In [14], electrical modularity is proposed with a modified electrical coupling strength (ECS) matrix as a substitute for adjacency matrix. In this paper, EEB will replace the elements in adjacency matrix as is shown below in (10) and (11), where E is the matrix of EEB.

$$Q = \sum_{v,w\in B}\left[\frac{E_{v,w}}{2M} - \frac{E_v}{2M}\frac{E_w}{2M}\right]\cdot\delta(C_v, C_w) \tag{9}$$

$$M = \frac{1}{2}\sum_{v,w}E_{v,w} \tag{10}$$

where $E_{v,w}$ is the v_{th} row and w_{th} column in matrix E, and E_w is the sum of all betweenness connecting with node w, which is the sum of w_{th} row and w_{th} column, minus $E_{w,w}$.

In Newman's method [2], community border is the edge with highest betweenness, to maximize the heterogeneity of graph. On contrary, our research suggests that to ensure ADN self-sufficiency, the lines with least EEB should be removed first as the border lines and form cluster based on remaining lines. Thus, IGNA is proposed and will be explained below in part B.

3.2. Active Planning with Coupled Partitioning and Allocation

In ADN, VM could take up the role of agent for controlling ADN. As mentioned, in our proposed method, IGNA will be

implemented to determine the cluster of VMs as electrical communities. The notion of GNA is proposed in [2] where modularity Q is used for measuring the quality of network division.

Compared with GNA where line with highest edge betweenness is removed by iteration, IGNA removes the lowest EEB edges. It is believed that in conventional topological community, boundary edges between communities have higher edge betweenness, since the connection is sparser. However, in electrical network, all paths participate in energy transmission, instead of only the shortest path. A shorter electrical distance and a higher line capacity leads to a higher electrical edge betweenness and stronger connection. Thus, when a line EEB is higher, it should be more likely to be contained in one community; while when EEB is lower, that line is more prone to work as boundary between communities.

As mentioned, in IGNA, the number of ADN partition with the highest modularity is chosen for dynamic partition. The pseudocode of IGNA is shown in Algorithm 1.

Algorithm 1 Inversed Girvan Newman Algorithm

1. For every edge in graph, electrical betweenness is calculated.
2. Remove the edge with lowest electrical edge betweenness, randomly remove one if identical betweenness detected.
3. For remaining graph, electrical betweenness is calculated.
4. Repeat step 2 and 3 until all edges have been removed.
5. Partition finished by selecting the number of VMs with the highest modularity

In active planning of ADN with VMs, many features related with VM boundary will be more accurate if these factors are dynamically evaluated. In the meantime, if the allocation plan of DG and DESS resources are varied, EEB will be different and lead to a different partition result. Hence, partitioning should be coupled with resources allocation in the optimization process, rather than use a constant predefined partition.

An illustration of the proposed planning method is shown below in Fig. 2, where power system configurations (including DG and DESS resources allocation represented by a generation of genetic algorithm solution) are converted into a graph which is represented by an EEB square matrix, with the size of number of nodes. Then through IGNA with newly defined EEB, the partition result is given to discover the communities, or rather VMs, in ADN. This result will be evaluated by implementing Monte-Carlo Simulations (MCS) for better representing the uncertainty in ADN. Genetic Algorithm (GA) has the decision variables of DG and DESS location, capacity, and type. Then, the evaluation will be sorted and selected in GA to produce child generation. The new GA child generation (representing new solution for resources allocation) will go through aforementioned process iteratively, until convergence or reached maximum generations. The pseudocode is shown in Algorithm 2.

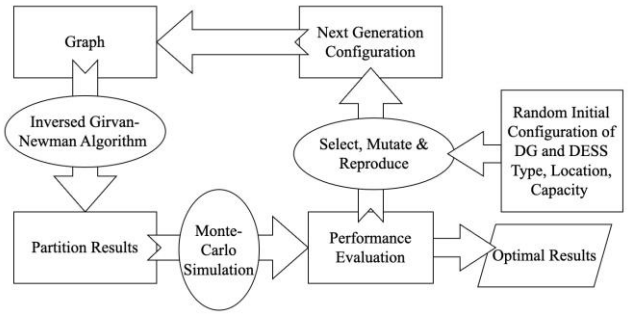

Fig. 2 Implementation of Coupling Partition and Configuration Planning in Genetic Algorithm

Algorithm 2 Proposed Active Planning Procedure

· generate Initial Population Chromosome Group $\mathcal{X}$
· generate MATPOWER case
for $\boldsymbol{j}$ from 1 to maximum generations:
  for $\boldsymbol{i}$ from 1 to GA population size:
    for $\boldsymbol{t}$ from 1 to MCS sampling size:
      · generate a graph containing configuration and partition information
      · generate graph's EEB matrix, determined by DG configuration
      · partition system using Algorithm 1, return $\boldsymbol{\mathcal{P}}$
      evaluate objectives based on $\boldsymbol{\mathcal{P}}$ and $\boldsymbol{X}$
    end MCS
  · select best population as parents
  · randomly mutate genome
  · generate kids as next parent generation
  end $\boldsymbol{j_{th}}$ generation
  if fitness function deviation ≤ tolerance
    · break loop
  end if
end GA
· return population
· plot Pareto Front and choose the knee point $\boldsymbol{X}$
· convert $\boldsymbol{X}$ to MATPOWER case for further study

3.3. Bi-level Optimization

In this paper, optimal planning of ADN is implemented by bi-level multi-objective optimization, where the outer layer of optimization is responsible of deploying both dispatchable and non-dispatchable DGs and DESSs in ADN, and the inner optimization takes the role of calculating the minimal operation cost of aforementioned deployment. A detailed diagram of the bi-level optimization is shown in Fig. 3.

The first optimization objective in outer layer is a combined cost, consisting of both operational cost, installation cost, and penalty cost for boundary flow. As the increase in generator capacity leads to better network features, such as self-sufficiency and flexibility supply, purchase cost is added to avoid excessive DG installation.

$$Obj_1 = min \sum_{G} (f_o(g) + f_i(g)) + \sum_{B} f_p(b) \qquad (11)$$

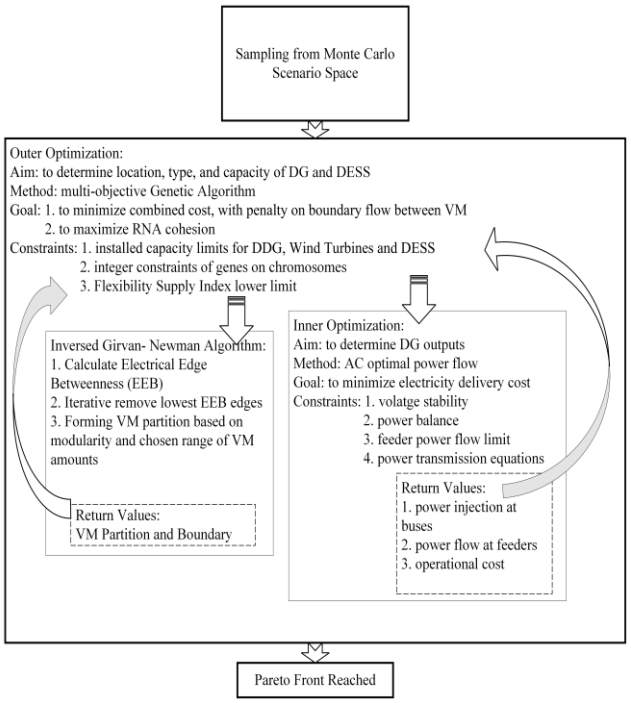

Fig. 3 Bilevel Optimization

$f_o(g)$ is the operational fuel cost. $f_i(g)$ is the purchase cost. Note that DG purchase is one time expenditure, so in optimization, it is levelized in one time step, considering DG and DESS service time. $f_p(b)$ is the penalty fee for VM boundary line flow, related to the partition results. It is useful in restraining boundary flow and ensuring VM self-sufficiency.

The second optimization objective of outer layer optimization includes cohesion of flexibility supply index and revised net-ability. This objective is designed for bettering network performance. With higher cohesion in RNA and FSI, VMs work better as partition than combined.

$$Obj_2 = max\ CI(X|\mathcal{S}, s) \tag{12}$$

$$CI(X) = \frac{1}{N_m}\left(\sum_V RNA_i(X) - RNA_{tot}(X)\right) \tag{13}$$

$$RNA = CF \cdot FSI \cdot \frac{1}{N_G N_D}\sum_{\mathcal{G}}\sum_{\mathcal{D}}\frac{C_{ij}}{Z_{ij}} \tag{14}$$

$$CF = \frac{\sum_{\Gamma} C_{G_i}}{\sum_{\mathcal{D}} L_i} \tag{15}$$

where $CI(X|\mathcal{S}, s)$ is the cohesion intensity of the given chromosome X. $\mathcal{S}$ stands for the system and s is the set of subsystems in $\mathcal{S}$, representing how $\mathcal{S}$ is partitioned. RNA is the revised net-ability considering capacity factor CF. FSI is the flexibility supply index. C_{ij} is the capacity from generator i in set $\mathcal{G}$ to load j in set $\mathcal{D}$. Z_{ij} is the corresponding equivalent impedance. This item $\frac{1}{N_G N_D}\sum_{\mathcal{G}}\sum_{\mathcal{D}}\frac{C_{ij}}{Z_{ij}}$ is the original definition of net-ability (NA) [29] and in this research, it is extended for modelling capacity fitness and flexibility supply. The calculation of FSI will be explained below in Section 3.4.

Capacity Fitness (CF) is defined as the ratio between the sum of DG capacity C_{G_i} and sum of load capacity L_i in VM i and in the whole ADN.

3.4. Flexibility Supply Index

Based on previous research [19], flexibility is represented by system ramp rate capacity, available power, and energy provision capacity, considering both upwards and downwards. Upwards are defined as the increase in power supply or decrease in power demand. Downwards is defined as the decrease in power supply or increase in power demand. Each planned component in ADN will be assessed regarding their flexibility and forming a Flexibility Array (FA) in predicted scenario s as,

$$FA_s = \left[F_{ramp+}, F_{ramp-}, F_{power+}, F_{power-}, F_{energy+}, F_{energy-}\right] \tag{16}$$

Similarly, to enable comparison between flexibility supply and uncertainty levels, Uncertainty Array (UA) in predicted scenario s is designed as,

$$UA_s = \left[U_{ramp+}, U_{ramp-}, U_{power+}, U_{power-}, U_{energy+}, U_{energy-}\right] \tag{17}$$

In our research, Flexibility Supply Index (FSI) is quantified as the L^2 norm of the division array of FA and UA. calculated by Monte Carlo Simulation (MCS) via sampling.

$$FA_{MC}(\cdot) = \frac{1}{N_{iter}}\sum FA_s(\cdot)(\Omega_{scene}) \tag{18}$$

$$UA_{MC}(\cdot) = \frac{1}{N_{iter}}\sum UA_s(\cdot)(\Omega_{scene}) \tag{19}$$

$$FSI = norm\left(\frac{FA_{MC}(\cdot)}{UA_{MC}(\cdot)}\right) \tag{20}$$

Specifically, to calculate FA and UA of different components in ADN, the calculation of flexibility is different. In dispatchable DGs, the flexibility array is determined by DG's power output as is shown in the Table 1.

In DESS, flexibility quantification is different, with regard to the state of charge (SoC), which determines whether the DESS will be able to charge/discharge fully. Different values are given in charging ramp rate RR_c, charging power P_c and discharging ramp rate RR_{dc}, discharging power P_{dc}.

Table 1 Flexibility Supply Array of Dispatchable-DG and DESS

DESS SoC Range	Upward Flexibility	Downward Flexibility
$(\boldsymbol{SoC_{min}}, \boldsymbol{SoC_{min}} + \frac{\boldsymbol{P_{dc}T}}{\boldsymbol{E_m}}]$	$[RR_{dc}, \frac{E_m SoC}{T}, E_m SoC]$	$[RR_c, P_c, P_c T]$
$(\boldsymbol{SoC_{min}} + \frac{\boldsymbol{P_{dc}T}}{\boldsymbol{E_m}}, \boldsymbol{SoC_{max}} - \frac{\boldsymbol{P_cT}}{\boldsymbol{E_m}}]$	$[RR_{dc}, P_{dc}, P_{dc}T]$	$[RR_c, P_c, P_c T]$
$(\boldsymbol{SoC_{max}} - \frac{\boldsymbol{P_cT}}{\boldsymbol{E_m}}, \boldsymbol{SoC_{max}}]$	$[RR_{dc}, P_{dc}, P_{dc}T]$	$[E_m(SoC_{max} - SoC), \frac{E_m(SoC_{max} - SoC)}{T}, RR_c]$
Dispatchable DG Output	**Upward Flexibility**	**Downward Flexibility**
$\boldsymbol{P_g = P_{rate}}$	$[0, \ 0, \ 0]$	$[RR_g, P_{rate}, P_{rate}T]$
$\boldsymbol{0 < P_g < P_{rate}}$	$[RR_g, P_{rate} - P_g, (P_{rate} - P_g)T]$	$[RR_g, P_g, P_g T]$
$\boldsymbol{P_g = 0}$	$[RR_g, P_{rate}, P_{rate}T]$	$[0, \ 0, \ 0]$

Controllable loads (CL) also contribute to flexibility supply. CL is flexible and fast responsive, so it is more appropriate to deploy CL not in early planned stage in day-ahead market, but to utilize CL solely for flexibility supply in real-time market regulation. The flexibility array of CL is simply given as

$$Flex_{cl} = [RR_{cl}^{+}, RR_{cl}^{-}, P_{cl}^{+}, P_{cl}^{-}, P_{cl}^{+}T, P_{cl}^{-}T] \quad (21)$$

where $RR_{cl}^{\pm}$ is the charging/discharging ramp rate, and $P_{cl}^{\pm}$ is charging/discharging power of controllable loads.

Based on prediction of RES and load situation, what remains *uncertain* in system is the error in prediction. For wind prediction, the forecast error ε_w is given as

$$\varepsilon_w(t) = w(t) - \hat{w}(t) \quad (22)$$

where $w(t)$ is the real total wind output and $\hat{w}(t)$ is the predicted wind generation at time t based on historical data.

Thus, the uncertainty of wind is given by,

$$\mathbb{U}_{p,+,w} = \begin{cases} \varepsilon_w & \varepsilon_w > 0 \\ 0 & \varepsilon_w \le 0 \end{cases} \quad (23)$$

$$\mathbb{U}_{p,-,w} = \begin{cases} 0 & \varepsilon_w > 0 \\ \varepsilon_w & \varepsilon_w \le 0 \end{cases} \quad (24)$$

$$\mathbb{U}_{e,\pm,w} = \varepsilon_w * T \quad (25)$$

$$\mathbb{U}_{r,\pm,w} = \varepsilon_w / T \quad (26)$$

Similarly, if we define the total error of load prediction as

$$\varepsilon_l(t) = l(t) - \hat{l}(t) \quad (27)$$

Then the uncertainty of load is given by,

$$\mathbb{U}_{p,+,l} = \begin{cases} \varepsilon_l & \varepsilon_l > 0 \\ 0 & \varepsilon_l \le 0 \end{cases} \quad (28)$$

$$\mathbb{U}_{p,-,l} = \begin{cases} 0 & \varepsilon_l > 0 \\ \varepsilon_l & \varepsilon_l \le 0 \end{cases} \quad (29)$$

$$\mathbb{U}_{e,\pm,l} = \varepsilon_l * T \quad (30)$$

$$\mathbb{U}_{r,\pm,l} = \varepsilon_l / T \quad (31)$$

To conclude, the calculation process of FSI is illustrated in Fig. 4 below. FA are calculated in the setting of day-ahead market estimating flexibility supply, whereas UA represents real-time market and any deviation from forecast is viewed as *uncertain* and needs to consume flexibility and be cleared. By sampling from a Monte Carlo scenario space Ω_{scene}, FA is calculated based on system configuration, with the RES and load forecast as parameters. Then based on modelling of RES and load forecast error, UA is calculated and compared with FA to get FSI.

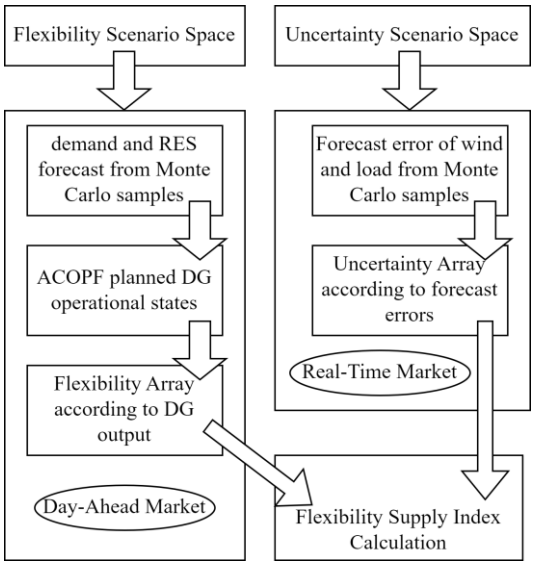

Fig. 4 Calculation of Flexibility Supply Index

3.5. Constraints

For the outer optimization, we have installed capacity limit, limiting algorithm from building excessive amount of DG and DESS for maximizing network efficiency in ADN.

$$\sum_{\Gamma_{DG}} C_{DG,i} \le C_{DG,max} \quad (32)$$

$$\sum_{\Gamma_{DESS}} C_{DESS,i} \le C_{DESS,max} \quad (33)$$

Also, to ensure each VM have enough CF, minimal installation is restricted to supply critical load.

$$\frac{\sum_{\Gamma_i} C_i}{\sum_{\Delta_i} L_i} \ge K_i \quad (34)$$

where K_i stands for the critical load percentage. L_i is the total load in VM i. C_i is the installed DG capacity in VM i.

To ensure enough renewable energy penetration in each VM, minimal wind power capacity is defined.

$$C_{WT,i} \ge C_{WT,i,min} \quad (35)$$

where $C_{WT,i}$ is the wind power installed capacity in VM i, and $C_{WT,i,min}$ is the lower bound.

Also, the minimal FSI limit in each VM is defined as

$$FSI_i \ge FSI_{i,min} \quad (36)$$

where $FSI_{i,min}$ is the lower limit.

For inner layer of optimization, constraints include:

- Power transmission equations

$$P_i = |V_i| \sum_{j=1}^{|B|} |V_j| \left(G_{ij} \cos(\delta_{ij}) + B_{ij} \sin(\delta_{ij})\right) \quad (37)$$

$$Q_i = |V_i| \sum_{j=1}^{|B|} |V_j| \left(G_{ij} \sin(\delta_{ij}) - B_{ij} \cos(\delta_{ij})\right) \quad (38)$$

- Power flow thermal limit on feeders

$$P_{ij} \leq P_{ij}^{max} \quad (39)$$

- Voltage stability

$$V_{i,min} \leq V_i \leq V_{i,max} \quad (40)$$

- Power balance equation

$$\sum_{\Gamma} P_{DG_i} = \sum_{\Delta} L_i + \sum_{B} TL_i \quad (41)$$

in which P_i and Q_i stand for active and reactive power injection at node i. V_i is bus i voltage, G_{ij} and B_{ij} are the admittance of branch i to j. δ_{ij} is the phasor angle difference between bus i and bus j.

4. Case Study

4.1. System Modelling

In this section, our proposed coupled active planning process is tested on the IEEE PG&E 69 bus radical system. The planning results are compared with static planning results, both in system self-sufficiency and in flexibility supply's cohesion.

In our case studies, wind power distribution is sampled and curve-fitted from the observatory data in Liverpool, UK by Weibull Distribution as is formulated by (42). The distribution and corresponding parameters are shown in Fig.5. A is the scale parameter, which is the expectation of Weibull Distribution, and k is the shape parameter.

$$f(v_{wind}) = \frac{k}{A}\left(\frac{v_{wind}}{A}\right)^{k-1} exp\left(-\left(\frac{v_{wind}}{A}\right)^{k}\right) \quad (42)$$

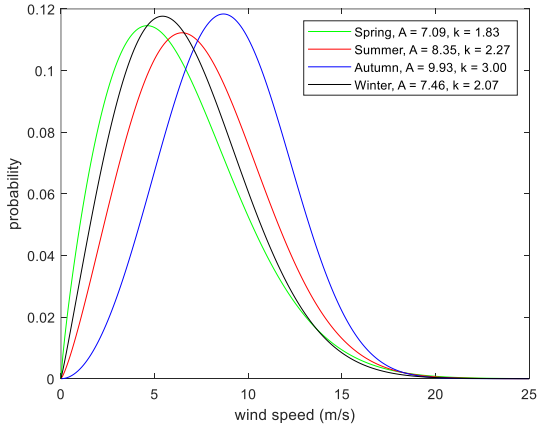

Fig. 5 Weibull Distribution of Wind Speed Across 4 seasons in Liverpool, UK.

Load distribution is categorized into 8 scenarios, which are weekdays/ends across four seasons based on IEEE Reliability testbench data [30].

The configuration of both dispatchable DGs and wind turbines are designed to four levels, either 50 kW, 100 kW, 150 kW, or 200 kW. DESS is defined with 50 kW charging/discharging power, with 120 kWh as the rated energy storage. Wind turbines are modelled by a cut-in wind speed as 2 m/s, rated output wind speed as 10 m/s, and cut-out wind speed as 20 m/s.

4.2. Coupled Configuration and Partition

For the implementation, MATLAB R2022a is used for coding. The ACOPF is carried out by MATPOWER 7.0 [31]. The pareto front of bilevel optimization is shown below in Fig 6, indicating the trade-off between cost and RNA and FSI Cohesion.

The coupled configuration and partitioning results corresponding to the knee points, which is the point on Pareto Front where the improvement on one objective leads to the least deterioration on other objectives, are shown in Fig. 7. The capacity of each bus's DG is shown in Fig 8.

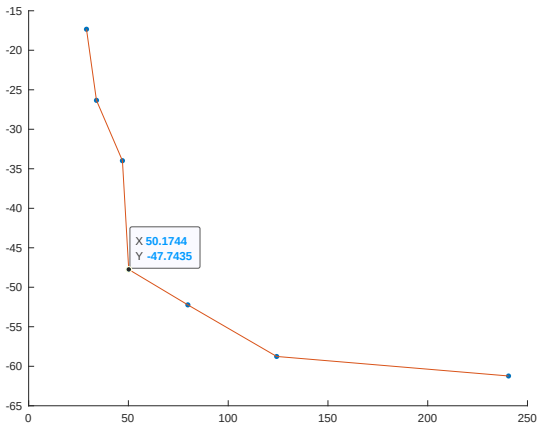

Fig. 6 Pareto Front of Bilevel Optimization and Knee Point

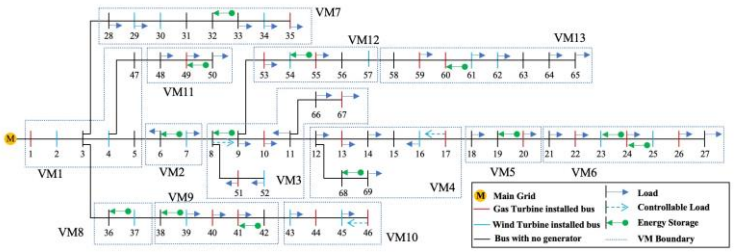

Fig. 7 Planning Result with Coupled Partition and Configuration

The partition scheme shown in Fig. 7 is the result of Inverse-Girvan-Newman Algorithm and the relationship between VM partition number and modularity is shown in Fig. 9. Modularity peaked at 13 VM partitions in the PG&E 69 bus system.

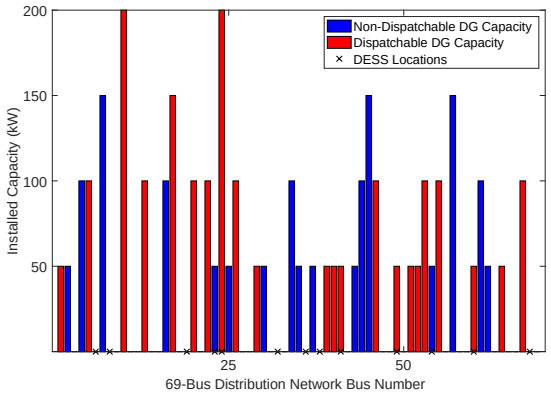

Fig. 8 Configuration Results on IEEE 69-bus Test System

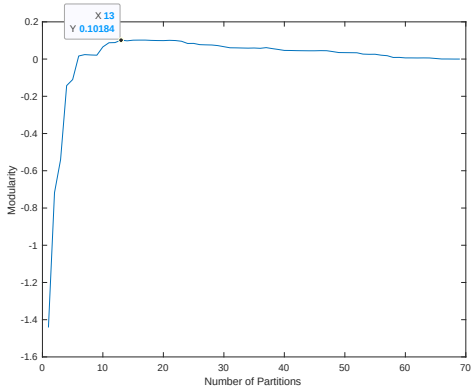

Fig. 9 Partitioning Results Analysed by Number of Communities.

4.3. Comparison

Firstly, to verify the solidarity of the coupled-configuration-partition active planning, a comparison between static planning method and the proposed planning method is made. The static planning [14] utilized partition scheme as predefined by pure structural analysis, without considering resources allocation, with identical optimization constraints. The process difference between static planning and coupled-configuration-partition active planning is shown in Fig. 10.

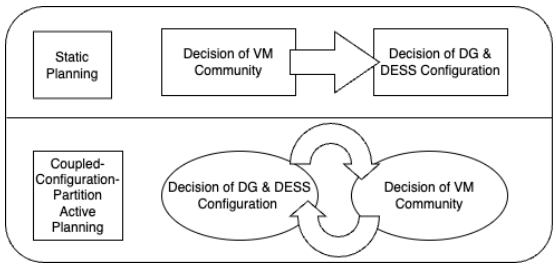

Fig. 10 Difference between two active planning mechanism in case study.

The results of static planning are shown in Table 2. and Fig. 11 below. It is noticed that the proposed coupled method has better performance (denoted by asteroids) in CI, operational cost, power from main grid, and modularity, showing a better self-sufficiency and a better cohesiveness in ADN partition. FSI and RNA cohesion is also much higher than static planning, indicating the coupled active planning discovered and utilized cohesive features much better than in static boundary case. The average boundary flow is a little bit higher (but still at close level) in coupled-configuration-partition method, possibly due to more interaction among VMs and less total installation. Note that if local implementation capacity is high enough, the power bought from main grid could be reduced to zero, representing better self-sufficiency in the coupled planning case.

The flexibility of coupled-configuration-partition is shown below in Table 3. Compared with the static border planning scenario, it is noted that the proposed result yields better flexibility supply index other than $F_{ramp}{}^{-}$. The most salient improvement is the ramp rate, due to more DESS are installed, which provides ramp rate flexibility support.

To sum up, when considering the coupling between configuration and partition, the result is better in flexibility supply, self-sufficiency, partition cohesive intensity, and

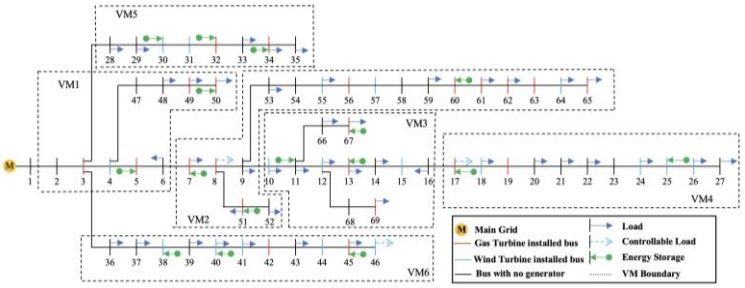

Fig. 11 Static Boundary Planning

modularity.

To further explore the partition effectiveness, we designed a case study where the boundaries are detected by original definition of edge betweenness [32], using conventional GNA instead of IGNA, where the highest betweenness is removed. Total 7 partitions are made and new boundary at bus 3-4, 3-36, 8-9, 11-12, 56-57,18-19 are generated, as is shown in Fig.12. The comparison is shown below in Table 4.

Table 2. Comparisons between Partition-Coupled and Static Boundary Active Planning.

Boundary	**Configuration-Partition-Coupled**	**Static**
Operational Cost ($/hr)	50.1744*	57.48
FSI & RNA Cohesion	47.7435*	11.489
Average Boundary Flow (MW)	0.2962	0.2640*
Main Grid Power (MW)	0*	0.30
Modularity	0.1018*	0.1009

Table 3. Flexibility Supply Index of CCP-AP and Static Boundary Planning.

	$F_{ramp}{}^{+}$	$F_{ramp}{}^{-}$	$F_{pwr}{}^{+}$	$F_{pwr}{}^{-}$	$F_{engr}{}^{+}$	$F_{engr}{}^{-}$
Coupled-Configuration-Partition	53.67*	22.61	10.29*	6.16	11.72*	5.85*
Static Planning	23.33	26.13*	9.56	8.89*	9.78	4.45

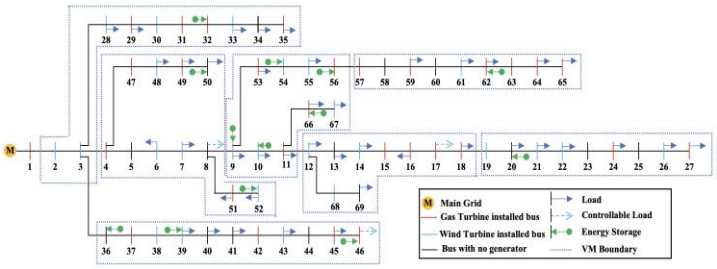

Fig. 12 Comparative Case from conventional GNA Partition

Comparing proposed EEB and conventional edge betweenness, based on the same DG and DESS allocation, it is observed that partition using proposed EEB will yield better FSI and RNA cohesion, and less boundary flow, indicating the VM system is more self-sufficient and cohesive.

Table 4. Comparisons between partitions based on proposed coupled active planning and conventional GNA method.

Planning Scheme	IGNA	Conventional GNA
No. of Partitions	13	7
FSI & RNA Cohesion	47.7435*	30.7822
Average Boundary Flow (MW)	0.2962*	0.5960

Furthermore, the result of CCP-AP process may be seriously related with the available RES energy resources. So, another case study is carried out to check the sensitivity of CCP-AP regards to different wind resource scenarios.

The comparison with new result based on a decreased wind supply is given in Table 5. The average wind speed, i.e., the scale parameter, in Weibull distribution is decreased by half while the shape parameter, denoting the variation, remains. When applied this to different scenarios, the operational cost increased significantly as the wind resource decrease and FSI cohesion intensity decreased, due to more widely spread wind turbines. Total wind turbine installed increased because of active planning intend to exploit more wind power from a deduced wind scenario. The increase of boundary flow and main grid power also reflect the decrease in system cohesion and self-sufficiency.

Table 5. Comparison between real wind speed and reduced wind speed scenario.

Average Wind Speed	Normal	Reduced 50%
Operational Cost ($/hr)	50.1744*	64.2324
FSI & RNA Cohesion	47.7435*	12.14
Wind Turbine Installed Capacity (GW)	3.05	4.15
Average Boundary Flow (MW)	0.2962*	0.7615
Main Grid Power (MW)	0*	0.2431
Modularity	0.1018	0.1024*

5. Discussion

5.1. Technical Standards Alignments

Proposed CCP-AP method can be integrated into industry conventions and practices. The proposed methodology aligns with existing technical standards, such as IEEE Std 1547.4-2011 [33] and IEEE Std 2030-2011 [34], which provide guidelines for the interconnection and operation of microgrids. Virtual Microgrid can operate as the building blocks of active distribution systems defined in [33].CCP-AP process determines the optimal placement and operation of DERs within local EPS. By defining clear VM boundaries and ensuring cohesive operation within those boundaries, this method enhances the interoperability between different DERs and the grid.

Virtual Microgrid, as well as its boundary and asset placement decision process, can be applied in smart grid agenda. In [34], the guidelines for smart grid architectural principles are provided, which includes considerations for integrating DERs within the grid. As mentioned before, CCP-AP allows the expansion of ADN when the topology changes, which showed the extensibility, scalability, and interoperability.

In summary, our approach followed these standards by offering an accurate and versatile planning strategy, that ensures VM self-sufficiency and optimal resource allocation, addressing key aspects of microgrid interoperability as mentioned in IEEE guidelines.

5.2. Decarbonization, Decentralization, and Digitalization

Decarbonization, Decentralization, and Digitalization (3-Ds) are viewed as the target towards which future power network is evolving [35]. The CCP-AP methods proposed in this research paper showed potential applications in the 3-Ds of ADN.

First, with the increased scale of RES in global decarbonization agenda, future ADN is required to accommodate new DER as an integral part of the grid, enhancing its flexibility and self-sufficiency. With sufficient flexibility supply in VM and in ADN, the system can accommodate more RES which is fluctuating, and hence will reduce the need to RES curtailment.

Also, the decentralization control of power system relies on the correct boundary of power system market agent. As is shown in the case studies, CCP-AP partitioned system has higher cohesion under lower operational cost, compared with predefined boundary case. This provides a better foundation of system decentralized control.

In 2022, European Commission proposed the framework [36] in digitalization, including the action to identify the digital tools in P2P energy exchange for energy communities. Based on VM as market participants, the Transactive Energy Management (TEM) can be achieved by digital quantified methods, such as smart contracts for automated energy trading, blockchain technology for secure and transparent transactions, and machine learning algorithms for system forecasting.

6. Conclusions

To conclude, a novel coupled-configuration-partition of active planning process is design and implemented in this paper with bi-level optimization. The definition of cohesion and cohesion intensity (CI) are given, to model the performance of VM partitioned ADN. During the optimization process under VM partitioned setting, operational cost, and CI of FSI and RNA are viewed as two objectives.

To assess those two objectives more accurately, and to include the variation of DG and DESS allocation, partition process is coupled in active planning. The graph partition is implemented by Inverse Girvan-Newman Algorithm, with newly designed electrical edge betweenness, representing each line's corresponding equivalent impedances and line capacity.

The optimization results are test in a case study, in which the improvement and effectiveness are examined. We can draw a conclusion that the proposed method has an edge in operational cost, system cohesion, modularity, and self-sufficiency. In this way, active management process is represented in active planning, by inclusion of RNA and FSI.

As mentioned, the lack of combination between defining partition and configuration in previous studies, neglecting the varying spatial features, are complemented by proposed method. Also, the quantification of flexibility supply is utilized in the planning procedure as the temporal features of optimization objectives.

In future studies, the potential smart contracts among VMs energy trading [37] can be utilized to perform TEM, as well as defensive strategies in emergency scenarios, with the resources defined by CCP-AP. Also, the inclusion of optimal planning SOP and ADN expansion can be adapted into CCP-AP, enabling the graph topology to vary during planning process and finally improving network structure, where conventional methods such as [38-41] often neglect.

ACKNOWLEDGMENT

Funding: This work was partially supported by the project of the National Natural Science Foundation of China (52377117), the XJTLU Research Development Fund (RDF-18-01-04) and partially supported by the XJTLU AI University Research Centre, Jiangsu Province Engineering Research Centre of Data Science and Cognitive Computation at XJTLU and SIP AI innovation platform (YZCXPT2022103). (Corresponding author: Fei Xue)

REFERENCE:

[1] S. Chowdhury, S. P. Chowdhury, and P. Crossley, *Microgrids and active distribution networks*. 2009, pp. 1-298.

[2] M. E. J. Newman and M. Girvan, "Finding and evaluating community structure in networks," *Physical Review E - Statistical, Nonlinear, and Soft Matter Physics*, vol. 69, no. 2 2, pp. 1-16, 2004, doi: 10.1103/PhysRevE.69.026113.

[3] M. Biserica, G. Foggia, E. Chanzy, and J. C. Passelergue, "Network partition for coordinated control in active distribution networks," *2013 IEEE Grenoble Conference PowerTech, POWERTECH 2013*, pp. 1-5, 2013, doi: 10.1109/PTC.2013.6652277.

[4] Y. Chai, L. Guo, C. Wang, Z. Zhao, X. Du, and J. Pan, "Network Partition and Voltage Coordination Control for Distribution Networks With High Penetration of Distributed PV Units," *IEEE Transactions on Power Systems*, vol. 33, no. 3, pp. 3396-3407, 2018, doi: 10.1109/TPWRS.2018.2813400.

[5] H. Ruan, H. Gao, Y. Liu, L. Wang, and J. Liu, "Distributed Voltage Control in Active Distribution Network Considering Renewable Energy: A Novel Network Partitioning Method," *IEEE Transactions on Power Systems*, vol. 35, no. 6, pp. 4220-4231, 2020, doi: 10.1109/TPWRS.2020.3000984.

[6] P. Li, C. Zhang, Z. Wu, Y. Xu, M. Hu, and Z. Dong, "Distributed Adaptive Robust Voltage/VAR Control with Network Partition in Active Distribution Networks," *IEEE Transactions on Smart Grid*, vol. 11, no. 3, pp. 2245-2256, 2020, doi: 10.1109/TSG.2019.2950120.

[7] B. H. Ettore Bompard, Marcelo Maseral, Enrico Pons, "Smart Grid as Multi-layer Interacting System for Complex Decision Makings," in *Networks of Networks: The Last Frontier of Complexity*, A. S. Gregorio D'Agostino Ed. Rome, Italy: Springer, 2014, pp. 187-202.

[8] M. E. Nassar and M. M. A. Salama, "Adaptive self-adequate microgrids using dynamic boundaries," *IEEE Transactions on Smart Grid*, vol. 7, no. 1, pp. 105-113, 2016, doi: 10.1109/TSG.2015.2420115.

[9] M. Z. Oskouei, B. Mohammadi-Ivatloo, O. Erdinc, and F. G. Erdinc, "Optimal Allocation of Renewable Sources and Energy Storage Systems in Partitioned Power Networks to Create Supply-Sufficient Areas," *IEEE Transactions on Sustainable Energy*, vol. 12, no. 2, pp. 999-1008, 2021, doi: 10.1109/TSTE.2020.3029104.

[10] M. Barani, J. Aghaei, M. A. Akbari, T. Niknam, H. Farahmand, and M. Korpas, "Optimal partitioning of smart distribution systems into supply-sufficient microgrids," *IEEE Transactions on Smart Grid*, vol. 10, no. 3, pp. 2523-2533, 2019, doi: 10.1109/TSG.2018.2803215.

[11] S. A. Arefifar, Y. A. R. I. Mohamed, and T. El-Fouly, "Optimized multiple microgrid-based clustering of active distribution systems considering communication and control requirements," *IEEE Transactions on Industrial Electronics*, vol. 62, no. 2, pp. 711-723, 2015, doi: 10.1109/TIE.2014.2352212.

[12] S. A. Arefifar, Y. A. R. I. Mohamed, and T. H. M. El-Fouly, "Supply-adequacy-based optimal construction of microgrids in smart distribution systems," *IEEE Transactions on Smart Grid*, vol. 3, no. 3, pp. 1491-1502, 2012, doi: 10.1109/TSG.2012.2198246.

[13] J. Sardi, N. Mithulananthan, M. M. Islam, and C. K. Gan, "Framework of virtual microgrids formation using community energy storage in residential networks with rooftop photovoltaic units," *Journal of Energy Storage*, vol. 35, no. October 2020, pp. 102250-102250, 2021, doi: 10.1016/j.est.2021.102250.

[14] X. Xu, F. Xue, X. Wang, S. Lu, L. Jiang, and C. Gao, "Upgrading Conventional Distribution Networks by Actively Planning Distributed Generation Based on Virtual Microgrids," *IEEE Systems Journal*, pp. 1-12, 2020, doi: 10.1109/jsyst.2020.2999560.

[15] E. Lannoye, D. Flynn, and M. O'Malley, "Transmission, variable generation, and power system flexibility," *IEEE Transactions on Power Systems*, vol. 30, no. 1, pp. 57-66, 2015, doi: 10.1109/TPWRS.2014.2321793.

[16] J. Ma, V. Silva, R. R. Belhomme, D. S. Kirschen, and L. F. Ochoa, "Evaluating and Planning Flexibility in

Sustainable Power Systems," *IEEE Transactions on Sustainable Energy*, vol. 4, no. 1, pp. 200-209, 2013, doi: 10.2514/5.9781600862403.0469.0510.

[17] K. Studarus and R. D. Christie, "A deterministic metric of stochastic operational flexibility," 2013: IEEE, pp. 1-4, doi: 10.1109/PESMG.2013.6672534.

[18] Y. V. Makarov, C. Loutan, J. Ma, and P. de Mello, "Operational impacts of wind generation on California power systems," *IEEE Transactions on Power Systems*, vol. 24, no. 2, pp. 1039-1050, 2009, doi: 10.1109/TPWRS.2009.2016364.

[19] A. Ulbig and G. Andersson, "Analyzing operational flexibility of electric power systems," *International Journal of Electrical Power and Energy Systems*, vol. 72, pp. 155-164, 2015, doi: 10.1016/j.ijepes.2015.02.028.

[20] M. A. Bucher, S. Delikaraoglou, K. Heussen, P. Pinson, and G. Andersson, "On quantification of flexibility in power systems," *2015 IEEE Eindhoven PowerTech, PowerTech 2015*, 2015, doi: 10.1109/PTC.2015.7232514.

[21] V. Latora and M. Marchiori, "Efficient behavior of small-world networks," *Physical Review Letters*, vol. 87, no. 19, pp. 198701-1-198701-4, 2001, doi: 10.1103/PhysRevLett.87.198701.

[22] R. Li, W. Wang, Z. Chen, J. Jiang, and W. Zhang, "A review of optimal planning active distribution system: Models, methods, and future researches," *Energies*, vol. 10, no. 11, 2017, doi: 10.3390/en10111715.

[23] D. J. Vergados, I. Mamounakis, P. Makris, and E. Varvarigos, "Prosumer clustering into virtual microgrids for cost reduction in renewable energy trading markets," *Sustainable Energy, Grids and Networks*, vol. 7, pp. 90-103, 2016, doi: 10.1016/j.segan.2016.06.002.

[24] M. Khorasany, D. Azuatalam, R. Glasgow, A. Liebman, and R. Razzaghi, "Transactive energy market for energy management in microgrids: The Monash microgrid case study," *Energies*, vol. 13, no. 8, pp. 1-23, 2020, doi: 10.3390/en13082010.

[25] M. Girvan and M. E. J. Newman, "Community structure in social and biological networks," *Proceedings of the National Academy of Sciences of the United States of America*, vol. 99, no. 12, pp. 7821-7826, 2002, doi: 10.1073/pnas.122653799.

[26] P. Hines and S. Blumsack, "A centrality measure for electrical networks," *Proceedings of the Annual Hawaii International Conference on System Sciences*, no. January 2008, 2008, doi: 10.1109/HICSS.2008.5.

[27] Z. Wang, A. Scaglione, and R. J. Thomas, "Electrical centrality measures for electric power grid vulnerability analysis," *Proceedings of the IEEE Conference on Decision and Control*, no. January 2011, pp. 5792-5797, 2010, doi: 10.1109/CDC.2010.5717964.

[28] E. Bompard, D. Wu, and F. Xue, "Structural vulnerability of power systems : A topological approach," vol. 81, pp. 1334-1340, 2011, doi: 10.1016/j.epsr.2011.01.021.

[29] S. Arianos, E. Bompard, A. Carbone, and F. Xue, "Power grid vulnerability: A complex network approach," *Chaos*, vol. 19, no. 1, pp. 1-6, 2009, doi: 10.1063/1.3077229.

[30] P. F. Albrecht *et al.*, "IEEE RELIABILITY TEST SYSTEM," *IEEE Transactions on Power Apparatus and Systems*, vol. PAS-98, no. 6, pp. 2047-2054, 1979.

[31] R. D. Zimmerman, C. E. Murillo-sánchez, and R. J. Thomas, "MATPOWER : Steady-State Operations , Systems Research and Education," *IEEE Transactions on Power Systems*, vol. 26, no. 1, pp. 12-19, 2011.

[32] M. E. J. Newman, "Fast algorithm for detecting community structure in networks," *Physical Review E - Statistical Physics, Plasmas, Fluids, and Related Interdisciplinary Topics*, vol. 69, no. 6, pp. 5-5, 2004, doi: 10.1103/PhysRevE.69.066133.

[33] *IEEE Guide for Design, Operation, and Integration of Distributed Resource Island Systems with Electric Power Systems, IEEE Std 1547.4™-2011*, I. S. C. C. 21, New York, USA, 2011.

[34] *IEEE Guide for Smart Grid Interoperability of Energy Technology and Information Technology Operation with the Electric Power System (EPS), End-Use Applications, and Loads, IEEE Std 2030-2011*, I. S. C. C. 21, New York, USA, 2011.

[35] M. L. Di Silvestre, S. Favuzza, E. Riva Sanseverino, and G. Zizzo, "How Decarbonization, Digitalization and Decentralization are changing key power infrastructures," *Renewable and Sustainable Energy Reviews*, vol. 93, pp. 483-498, 2018, doi: 10.1016/j.rser.2018.05.068.

[36] (2022). *Digitalising the energy system - EU action plan COM(2022) 552 final*. [Online] Available: https://eur-lex.europa.eu/legal-content/EN/TXT/PDF/?uri=CELEX:52022DC0552

[37] K. Anoh *et al.*, "Virtual microgrids: A management concept for peer-to-peer energy trading," *ACM International Conference Proceeding Series*, no. June, pp. 0-5, 2018, doi: 10.1145/3231053.3231096.

[38] A. Farzamnia, S. Marjani, S. Galvani, and K. T. T. Kin, "Optimal Allocation of Soft Open Point Devices in Renewable Energy Integrated Distribution Systems," *IEEE Access*, vol. 10, pp. 9309-9320, 2022, doi: 10.1109/access.2022.3144349.

[39] P. Kayal, S. Maji, and S. Samantaray, "Assessment of topological boundaries for microgrids in an active power distribution network during emergencies," *e-Prime - Advances in Electrical Engineering, Electronics and Energy*, vol. 6, 2023, doi: 10.1016/j.prime.2023.100292.

[40] H. Mubarak *et al.*, "Optimum Distribution System Expansion Planning Incorporating DG Based on N-1 Criterion for Sustainable System," *Sustainability*, vol. 13, no. 12, 2021, doi: 10.3390/su13126708.

[41] H. H. Wang and L. B. Shi, "Optimal distribution network expansion planning incorporating distributed generation," presented at the 2016 IEEE PES Asia-

Pacific Power and Energy Engineering Conference (APPEEC), 2016.